

## Research Article

# Miniaturized 38GHz Circular Substrate Integrated Waveguide Band Pass Filter using Low Temperature Co-Fired Ceramic Technology

<sup>1</sup>Zulkifli Ambak, <sup>1</sup>Hizamel M. Hizan, <sup>1</sup>Ahmad Ismat Abdul Rahim, <sup>1</sup>Azmi Ibrahim, <sup>1</sup>Mohd Zulfadli M. Yusoff, <sup>2</sup>Razali Ngah and <sup>3</sup>Syamsuri Yaakob

<sup>1</sup>Communication Technology, TM Research and Development Sdn Bhd,  
Lingkaran Teknokrat, 63000, Cyberjaya, Selangor,

<sup>2</sup>Wireless Communication Center, Faculty of Electrical Engineering, Universiti Teknologi  
Malaysia, 81310, Johor,

<sup>3</sup>Department of Computer and Communication System Engineering, Faculty of Engineering, Universiti  
Putra Malaysia, 43400 UPM Serdang, Selangor, Malaysia

**Abstract:** This study presents design approach for realizing miniaturized Substrate Integrated Waveguide (SIW) Band Pass Filter (BPF) using Low Temperature Co-fired Ceramic (LTCC) technology at TMRND's LTCC Lab. Design method for the SIW BPF is based on the circular cavity structure with four pole Chebyshev and operating at center frequency of 38 GHz. This SIW BPF is an important part of the Remote Antenna Unit (RAU) transceiver for the Radio over Fiber (RoF) system. Two types of circular SIW BPF have been designed and investigated in term of performance and structure size which are planar SIW BPF and compact SIW BPF. Both SIW BPF were developed using LTCC Ferro A6M materials with dielectric constant of 5.8, loss tangent of 0.002 and metallization of gold. The insertion loss for planar SIW BPF and compact SIW BPF were measured at 6.2 dB and 6.3 dB, respectively. The passband return losses for both types of the SIW BPF were measured at more than 10 dB. The size of the compact SIW BPF is  $6.94 \times 6.94 \text{ mm}^2$  meanwhile size for planar SIW BPF is  $12.15 \times 4.145 \text{ mm}^2$ . The size of the compact SIW BPF is reduced to nearly 10% compared to a planar SIW BPF structure.

**Keywords:** Band pass filter, LTCC, RAU, RoF, SIW

## INTRODUCTION

A band pass filter is a key component for passive element in Remote Antenna Unit (RAU) transceiver for Radio over Fiber (RoF) systems. Generally, RoF systems have some advantages, such as low-loss and high speed wireless and wireline data transmission over fiber links which support high speed multimedia services and high definition video. The millimeter wave (mm-wave) frequency is started from 30 to 300 GHz have received more attracted because of possible miniaturization of the analog components such as filter and antennas. Although it has been known for many decades, this technology has attracted significant interest from researcher, academia and industry when advances in silicon process technology and low cost integration solution in Hizan *et al.* (2014). Huge demand of the higher data-speeds and high bandwidth applications is increasing recently, such as point to point wireless communication was reported (Van Heijningen and Gauthier, 2004), wireless indoor

communication network (Dang *et al.*, 2007), radio over fiber (Yaakob *et al.*, 2014).

One of the main issue to realize the mm-wave radio system is related with cost effective packaging and the size of the mm-wave modules structure like filter modules and amplifier modules. The waveguide filters are widely used because of their high Q value, high power capability and outstanding selective. However, they are bulky, heavy and not suited for high density integration. The present microwave and mm-wave filters are bulky and heavily that give a significant limitation when it comes to fabrication. Several microwave filter have been reported with new innovative design on size reduction. There are many types of filter topologies and structures to realize miniaturized microwave and mm-wave filter such as Substrate Integrated Waveguide (SIW), Stub Loaded Resonator (SLR) and Stepped Impedance Resonator (SIR) as reported by Vidhya and Jayanthi (2013). Wu *et al.* (2003) introduced the substrate integrated circuit in 2003 which is the new concept for high-frequency

**Corresponding Author:** Zulkifli Ambak, Communication Technology, TM Research and Development Sdn Bhd, Lingkaran Teknokrat, 63000, Cyberjaya, Selangor, Malaysia

This work is licensed under a Creative Commons Attribution 4.0 International License (URL: <http://creativecommons.org/licenses/by/4.0/>).

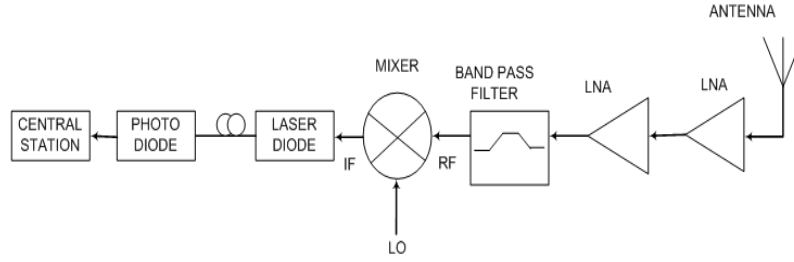


Fig. 1: Block diagram of the 38GHz RAU uplink for RoF systems

electronics and optoelectronics. Losses of SIW components are lower than the corresponding microstrip devices. In terms of size, SIW is more compact and easy to integrate with other microwave and millimeter-wave circuits in the same substrate compared to the conventional waveguide. SIW circuits are fabricated by application of either a standard Printed Circuit Board (PCB) or a Low Temperature Co-fired Ceramic (LTCC) process. Generally, the conventional structure of SIW filters are predominantly based on rectangular and circular cavities as reported by Xu *et al.* (2013) and De Carlo and Tringali (2010).

In this study, in regard to miniaturized which combine performance of circular Substrate Integrated Waveguide (SIW) Band Pass Filter (BPF) using Low Temperature Co-fired Ceramic (LTCC) technology was proposed. Design method for the SIW BPF is based on the circular cavity structure with four pole Chebyshev and operating at center frequency of 38 GHz. Two types of experimental SIW BPF structures at the same central frequency of 38 GHz are fabricated using Low Temperature Co-fired Ceramic (LTCC) technology. Design details are described and both simulated and experimental results are presented and discussed.

### SIW BAND PASS FILTER DESIGN

This study focuses on miniaturizing the circular Substrate Integrated Waveguide (SIW) band pass filter which will be employed as important part of the Remote Antenna Unit (RAU) for RoF applications as shown in Fig. 1. SIW band pass filter provides a low-profile, low-cost, possible integration and low-weight scheme while maintaining high performance, which is satisfied with the needs perfectly.

A basic structure of an SIW band pass with 1-pole Chebyshev characteristic was reported by Hizan *et al.* (2015) as shown in Fig. 2. The measured results of an insertion loss of -1.954 dB and the passband return loss of greater than 10 dB with 640 MHz bandwidth operating at 38 GHz.

In this study, a fourth order Chebyshev SIW BPF with 4 pole Chebyshev characteristic is designed and developed using in-house TMRND's LTCC technology. Two types of experimental SIW band pass filter structures have been designed and developed

which are planar SIW BPF as shown in Fig. 3 and compact SIW BPF as shown in Fig. 4. Table 1 shows the geometric dimension for both SIW BPFs.

The similar design technique as reported by Hizan *et al.* (2015) was applied. The filter's specification was shown in Table 2. However, in this design the number of order was changed from first degree Chebyshev to four orders for both filter types. The operating mode for the fourth order SIW filters are TM<sub>010</sub>. From the filter design theory in Hunter (2001) and Matthaie *et al.* (1980), the admittance inverter and capacitance values of the low pass prototype can be determined using the following formulas:

$$C_{\gamma} = \frac{2}{\eta} \sin \left[ \frac{(2\gamma-1)\pi}{2N} \right] \quad (1)$$

$$J_{\gamma,\gamma+1} = \frac{[\eta^2 + \sin^2(\gamma\pi/N)]^{1/2}}{\eta} \quad (2)$$

where, by N is the degree of the network and  $\eta$  is defined as:

$$\eta = \left[ \frac{1}{N} \sinh^{-1} \left( \frac{1}{\epsilon} \right) \right] \quad (3)$$

And  $\epsilon$  related to the insertion loss ripple and hence the passband return loss:

$$\epsilon = \left( 10^{\frac{LR}{10}} - 1 \right)^{-\frac{1}{2}} \quad (4)$$

The lowpass prototype is transformed into bandpass filter at 38 GHz centre frequency with -10 dB passband return loss bandwidth of 100 MHz. Under the transformation, the inverter values are invariant. Then, the lowpass prototype equivalent circuit can be transformed into a bandpass equivalent circuit using the formulas (5-7):

$$\alpha = \frac{f_0}{PBW} \quad (5)$$

$$L_1' = \frac{1}{\alpha C_1 \omega_0} \quad (6)$$

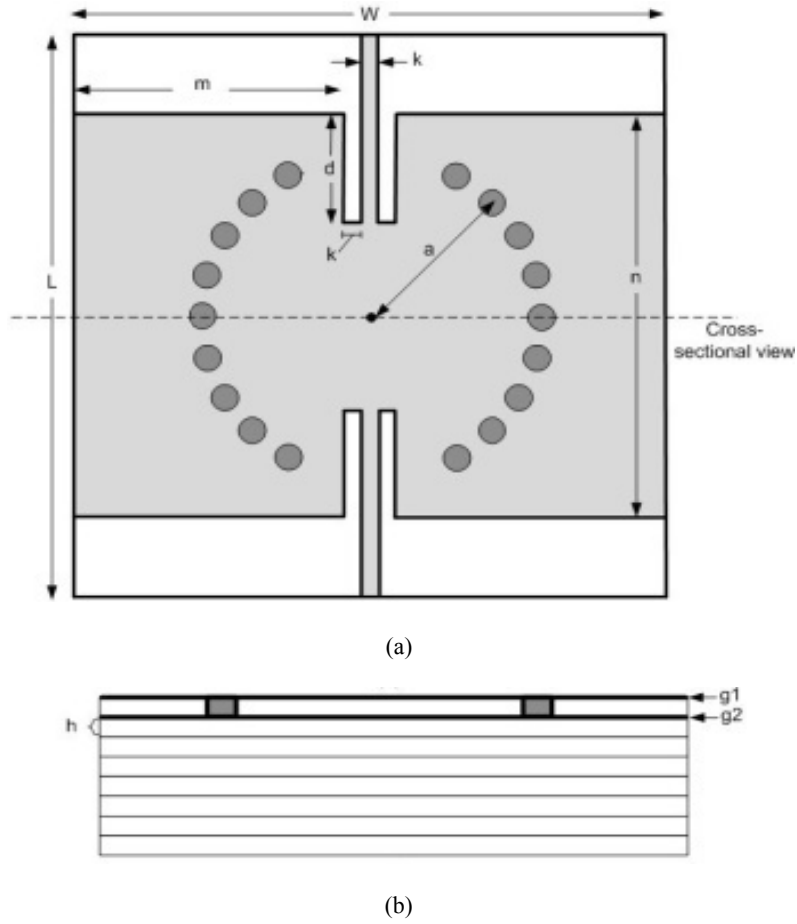


Fig. 2: (a) Top and (b) Cross-sectional views of first degree SIW band pass filter

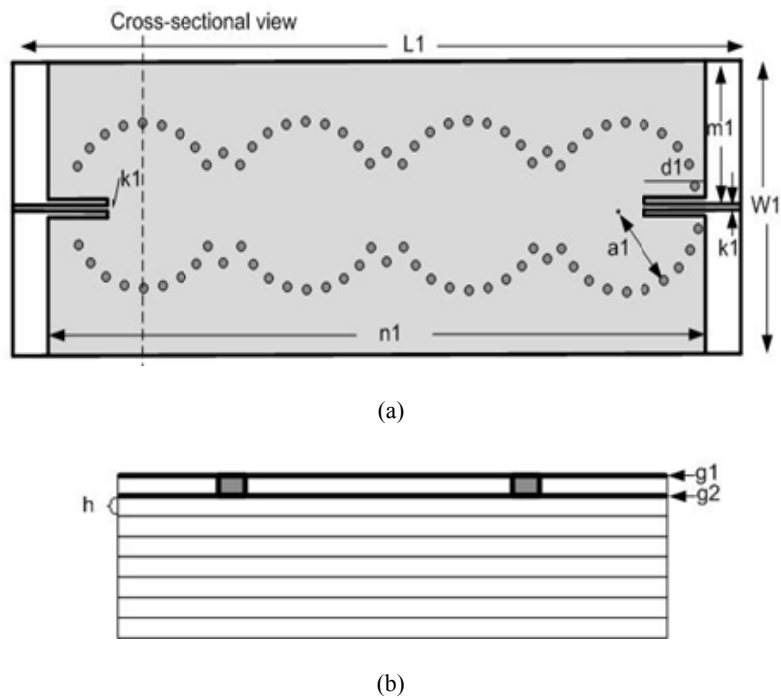


Fig. 3: (a) Top and (b) Cross-sectional views of planar SIW band pass filter

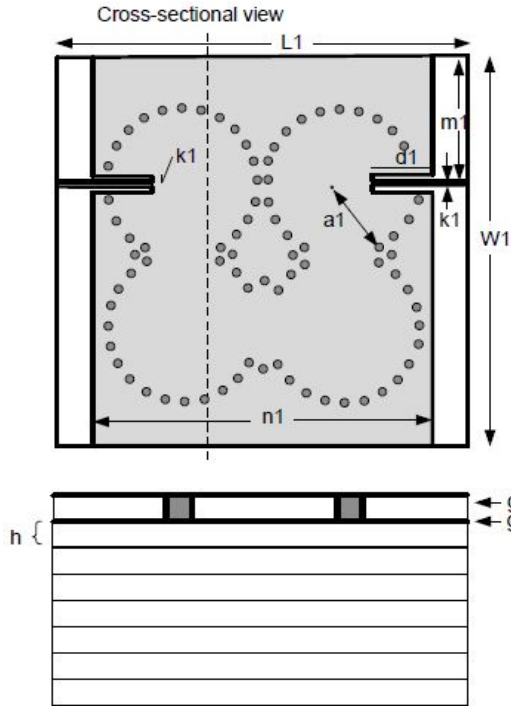


Fig. 4: (a) Top and (b) Cross-sectional views of compact SIW band pass filter

Table 1: Geometric dimension of the SIW BPFs  
Millimeter Wave SIW BPF

Degree/Pole symbol	1st Degree value (mm)	4rd Degree	
		Planar (mm)	Compact (mm)
k1	0.126	0.130	0.130
d1	0.850	0.922	0.922
n1	3.142	10.910	5.720
W1	4.382	4.345	6.940
L1	4.382	12.150	6.940
a1	1.261	1.261	1.261
m1	2.000	2.105	2.105
g1	0.010	0.010	0.010
g2	0.010	0.010	0.010
h	0.096	0.096	0.096

$$C_1' = \frac{\alpha C_1}{\omega_0} \quad (7)$$

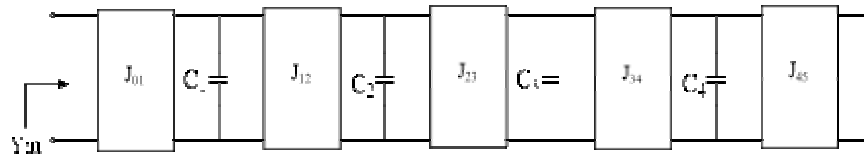


Fig. 6: Low pass prototype equivalent circuit of forth order planar SIW BPF

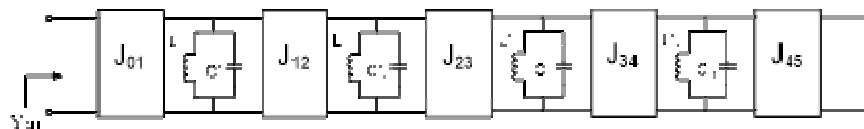


Fig. 7: Equivalent circuit of forth mode planar SIW BPF

Table 2: Specification of SIW band pass filter

Filter parameters	Value	Unit
Center frequency, $f_0$	38	GHz
Filter configuration	SIW	
Dielectric substrate	LTCC Ferro A6M	
Dielectric constant	5.9	
Size : Planar SIW	12.15×4.345	mm <sup>2</sup>
: Compact SIW	6.94×6.94	mm <sup>2</sup>
Passband Bandwidth (PBW)	2	GHz
Passband Return Loss (LR)	≥ 10	dB
Insertion loss	< 3	dB

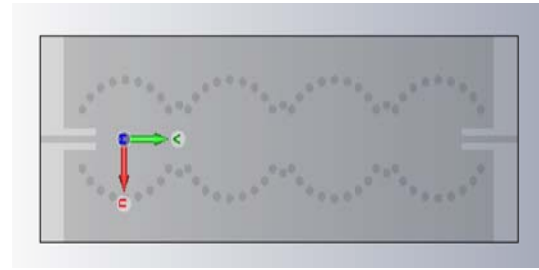


Fig. 5: Forth order planar SIW bandpass filter design

where, by  $\omega_0$  is the geometric midband frequency and  $\alpha$  is the bandwidth scaling factor. Figure 5 shows the planar SIW band pass filter. The forth order Chebyshev low pass equivalent circuit of planar filter is shown in Fig. 6. In this network, the admittance matrix, J01, J12, J23, J34 and J45 are used as the input and output coupling of the filter. The shunt capacitor, C1, C2, C3 and C4 are representing the n-mode resonator in the SIW cavity. Figure 7 shows the equivalent circuit of mm-wave planar circuit transformation from Fig. 6.

Figure 8 shows the compact SIW band pass filter. The Chebyshev low pass equivalent circuit of the compact filter is shown in Fig. 9. Meanwhile, Fig. 10 shows the equivalent circuit for compact band pass filter circuit transformation from Fig. 10.

### LTCC FABRICATED SIW BAND PASS FILTER

The SIW bandpass filter was fabricated using state-of-the art in-house TMRND's LTCC process as shown

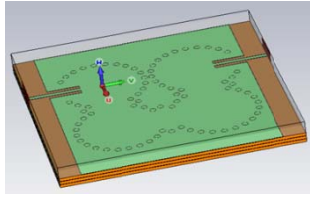


Fig. 8: Forth order compact SIW BPF design

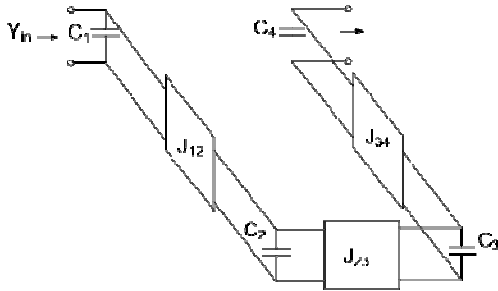


Fig. 9: Low pass prototype for forth order compact SIW BPF

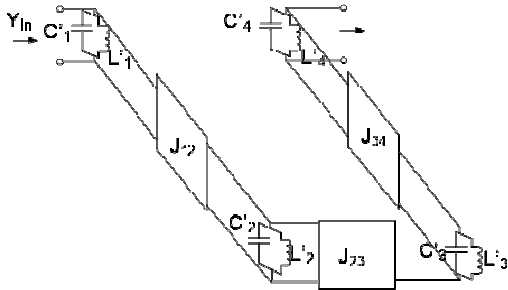


Fig. 10: Equivalent circuit for forth order compact SIW BPF

in Fig. 11. The overall LTCC process was mentioned by Hizan *et al.* (2015). The first step is the blanking process, which then proceeded to punching each via

hole of diameter 0.2 mm. Next, the via holes formed were filled with conductive compound. The SIW filter was screen-printed on the substrate and then proceeded to stacking the conductive layers together with the substrate layer. Upon completion of stacking, the laminating step was then initiated. Finally, the stacked and laminated layers were subjected to a co-firing process to form the SIW filter. The laminating pressure of 21 MPa and at 70°C was used, while the co-firing temperature was set at 850°C.

## RESULTS AND DISCUSSION

The simulated and measured responses of the design are compared in Fig. 12 and 13. The fabricated design is shown in Fig. 14. The design was tested using R&S ZVA50 network analyzer and Cascade Microtech 250 μm probe tips. The simulated results presented in Fig. 12 show the planar SIW BPF has centered at 38 GHz with insertion loss of 1.2 dB and return loss of 22.36 dB. The size of planar SIW BPF is 12.15×4.345×0.768 mm<sup>3</sup>. In the similar Fig. 12 shows the S<sub>21</sub> (dB) measured results of the planar SIW BPF that exactly centered at 38 GHz with the measured insertion loss of -6.2 dB and passband return loss, S<sub>11</sub>(dB) of 25.98 dB. The simulated results presented in Fig. 13 show the compact SIW BPF has centered at 38GHz with insertion loss of 1.13 dB and return loss of 20.1 dB. The size of planar SIW BPF is 6.94×6.94×0.768 mm<sup>3</sup>. Figure 13 shows the S<sub>21</sub>(dB) measured results of the compact SIW BPF that centered at 38 GHz with measurement insertion loss of 6.3 dB and passband return loss, S<sub>11</sub>(dB) of 16.74 dB. Both measurement insertion loss results are slightly higher than simulation results which is due to the loss tangent of material. A slight variation between measured and

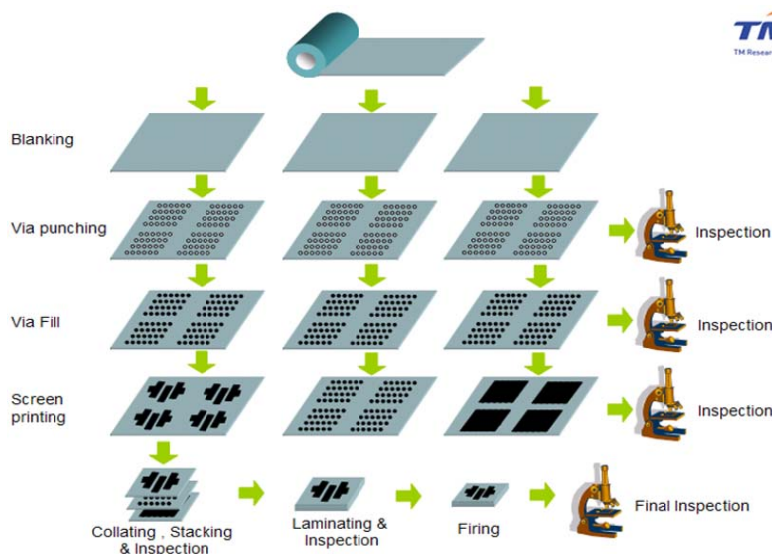


Fig. 11: TMRND's in-house LTCC process flow

Table 3: Comparison between the proposed design of circular SIW BPF and design proposed by Wang *et al.* (2010)

Filter parameters	(Wang <i>et al.</i> , 2010)	Proposed design compact SIW BPF
Center frequency, $f_0$	35.8	38
SIW Filter configuration	Cross coupled	Circular
Dielectric substrate	Ferro A6S	Ferro A6M
Dielectric constant	5.9	5.9
Size in $\text{mm}^3$	$9.5 \times 3.1 \times 1.3$	$6.94 \times 6.94 \times 0.768$
Passband Return Loss (LR), S11	14.85	16.7
Insertion Loss, S21	4.2	6.2

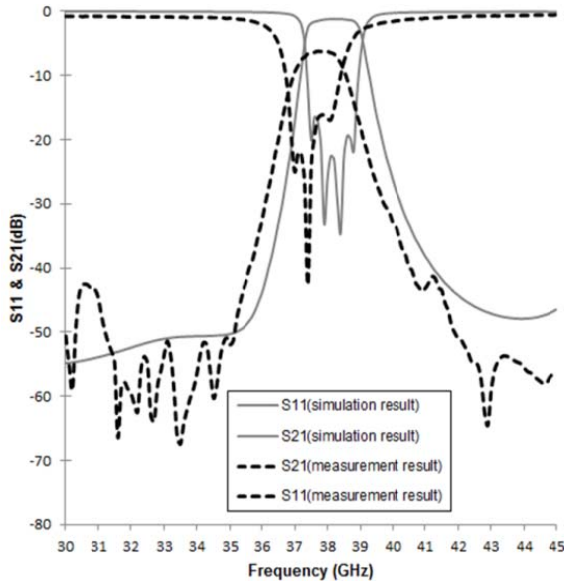


Fig. 12: Simulated and measured results for planar SIW BPF

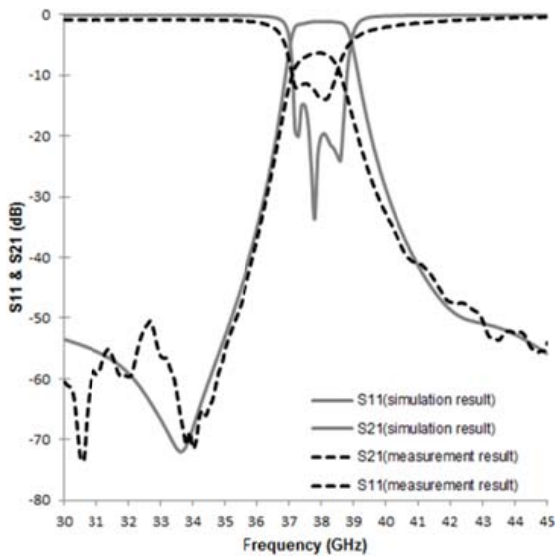


Fig. 13: Simulated and measured results for compact SIW BPF

simulated results observed at the stopband of the filter, between 39–46 GHz, was due the  $180^\circ$  input and output ports fabrication tolerance that induced the unwanted higher order modes of the structure during the LTCC process. The frequency shift may also be affected by the manufacturing tolerance.



Fig. 14: Photograph of the fabricated planar SIW BPF and compact SIW BPF at 38GHz

Table 3 shows the performance comparison between this study and proposed filter reported by Wang *et al.* (2010). There is different of the S-parameters result compared the proposed design of circular SIW. This is mainly caused by the inaccuracy in the characterization of relative permittivity and loss tangent of LTCC at 38 GHz. On the other hand, all metallic vias and metal surfaces are assumed to be perfectly conducting in our design, which will also result in the discrepancy in the measured and simulated in-band insertion losses. As shown, the proposed filter provides superior performance, particularly in a miniaturized compact SIW BPF.

### CONCLUSION

A miniaturized SIW bandpass filter using LTCC technology with 8 layers LTCC Ferro A6M has been presented in this study. The proposed planar and compact SIW BPF with 4 pole Chebyshev filter exhibits the passband of 37-39 GHz. Finally, the proposed planar and compact SIW BPF with four pole Chebyshev filter has been fabricated and measured. The overall size of the fabricated Planar SIW BPF is  $12.150 \text{ mm} \times 4.345 \text{ mm} \times 0.768 \text{ mm}$  meanwhile for compact SIW BPF is  $6.940 \text{ mm} \times 6.940 \text{ mm} \times 0.768 \text{ mm}$ . The measured insertion loss for compact SIW BPF at center frequency of 38 GHz is about 6.3 dB with the passband return loss better than 10 dB. Meanwhile, the measured insertion loss for planar SIW BPF is about 6.2 dB and passband return loss better than 10dB. It is shown that 10% miniaturized size reduction can be achieved with compact circular SIW BPF structure, compared to a planar SIW. This miniaturized SIW BPF is easy integrated with the other circuits in downlink/uplink remote antenna unit (RAU) for Radio over fiber system.

## REFERENCES

- Dang, B.L., M. Garcia Larrode, R. Venkatesha Prasad, I. Niemegeers and A.M.J. Koonen, 2007. Radio-over-fiber based architecture for seamless wireless indoor communication in the 60 GHz band. *Comput. Commun.*, 30(18): 3598-3613.
- De Carlo, D. and S. Tringali, 2010. Automatic design of circular SIW resonators by a hybrid approach based on polynomial fitting and SVRMS. *J. Electromagnet. Wave.*, 24(5-6): 735-744.
- Hizan, H.M., Z. Ambak, A. Ibrahim and M.Z. Mohamed Yusoff, 2014. Q-band millimeter-wave SIW filter using LTCC technology. *Proceeding of the IEEE Asia-Pacific Conference on Applied Electromagnetics (APACE)*. Johor Bahru, pp: 199-202.
- Hizan, H.M., Z. Ambak, A. Ibrahim, M.Z. Mohamed Yusoff and T. Kanesan, 2015. Effect of insertion losses on millimeter-wave SIW filters using LTCC technology. *Proceeding of the IEEE International RF and Microwave Conference (RFM)*. Kuching, pp: 65-68.
- Hunter, I.C., 2001. *Theory and Design of Microwave Filters*. The Institution of Electrical Engineers, London, United Kingdom.
- Matthaei, G.L., L. Young and E.M.T. Jones, 1980. *Microwave Filters, Impedance-matching Networks, and Coupling Structures*. Artech House, Dedham, Mass.
- Van Heijningen, M. and G. Gauthier, 2004. Low-cost millimeter-wave transceiver module using SMD packaged MMICs. *Proceeding of the 34th European Microwave Conference*. Amsterdam, The Netherlands, pp: 1269-1272.
- Vidhya, K. and T. Jayanthi, 2013. Design of folded multilayer microstrip tri-band hairpin band pass filter. *Res. J. Appl. Sci. Eng. Technol.*, 6(12): 2283-2287.
- Wang, Z., S. Bu and Z.X. Luo, 2010. A ka-band third-order cross-coupled substrate integrated waveguide bandpass filter base on 3D LTCC. *Prog. Electromagn. Res. C*, 17: 173-180.
- Wu, K., D. Deslandes and Y. Cassivi, 2003. The substrate integrated circuits - a new concept for high-frequency electronics and optoelectronics. *Proceeding of the 6th International Conference on Telecommunications in Modern Satellite, Cable and Broadcasting Service (TELSIKS, 2003)*. Nis, Yugoslavia, Yugoslavia, 1: 3-10.
- Xu, Z.Q., P. Wang, J.X. Liao and Y. Shi, 2013. Substrate integrated waveguide filter with mixed coupled modified trisections. *Electron. Lett.*, 49(7): 482-483.
- Yaakob, S., S.M. Idrus, N.M. Samsuri, M.Z. Abdul Kadir, R. Mohamad and M.A. Ismail, 2014. 40-GHz ROF downlink system with SFP modules. *Microw. Opt. Techn. Lett.*, 56(4): 900-903.